Electric Power Systems Research 113 (2014) 237–246

Contents lists available at ScienceDirect

Electric Power Systems Research

journal homepage: www.elsevier.com/locate/epsr

Interference from cloud-to-ground and cloud flashes in wireless communication system

Mohd Riduan Ahmad[a,b,*], Mona Riza Mohd Esa[a,c], Vernon Cooray[a], Eryk Dutkiewicz[d]

[a] Ångström Laboratory, Division for Electricity, Department of Engineering Sciences, Uppsala University, Box 534, S-75121, Sweden
[b] Universiti Teknikal Malaysia Melaka, Hang Tuah Jaya, 76100 Durian Tunggal, Malacca, Malaysia
[c] Universiti Teknologi Malaysia, 81310 Skudai, Johor Bahru, Johor, Malaysia
[d] Wireless Communications and Networking Lab, Department of Electronic Engineering, Macquarie University, Sydney, Australia

ARTICLE INFO

Article history:
Received 30 July 2013
Received in revised form 17 February 2014
Accepted 11 March 2014
Available online 13 April 2014

Keywords:
Bit error rate
Cloud flash
Cloud-to-ground flash
Interference
Microwave radiation
Wireless system

ABSTRACT

In this study, cloud-to-ground (CG) flash and intra-cloud (IC) flash events that interfere with the transmission of bits in wireless communication system operating at 2.4 GHz were analyzed. Bit error rate (BER) and consecutive lost datagram (CLD) measurement methods were used to evaluate BER and burst error from 3 tropical thunderstorms on November 27, 28, and 29 during 2012 northeastern monsoon in Malaysia. A total of 850 waveforms from the electric field change recording system were recorded and examined. Out of these, 94 waveforms of very fine structure were selected which matched perfectly with the timing information of the recorded BER. We found that both CG and IC flashes interfered significantly with the transmission of bits in wireless communication system. The severity of the interference depends mainly on two factors namely the number of pulses and the amplitude intensity of the flash. The interference level becomes worst when the number of pulses in a flash increases and the amplitude intensity of pulses in a flash intensifies. During thunderstorms, wireless communication system has experienced mostly intermittent interference due to burst error. Occasionally, in the presence of very intense NBP event, wireless communication system could experience total communication lost. In CG flash, it can be concluded that PBP is the major source of interference that interfered with the bits transmission and caused the largest burst error. In IC flash, we found that the typical IC pulses interfered the bits transmission in the same way as PBP and mixed events in CG flash and produced comparable and in some cases higher amount of burst error. NBP has been observed to interfere the bits transmission more severely than typical IC and CG flashes and caused the most severe burst error to wireless communication system.

1. Introduction

Wireless communication system has evolved rapidly from the last decade and utilized wide range of frequency bands for their operation particularly in the microwave region. Currently, broadband wireless systems (e.g. WiFi, WiMAX) are operating between 2 and 6 GHz frequency bands. Recent observations of microwave radiation from lightning flashes in [1,2] have triggered interest to study its effects on wireless communication system. The work in [1] has observed strong microwave radiation at 1.63 GHz associated with cloud-to-ground (CG) flash events such as preliminary breakdown process (PBP), stepped leaders (SLs), dart leaders (DLs), and return strokes (RSs). Moreover, similar microwave radiation at 2.4 GHz associated with cloud (IC) flash events such as narrow bipolar pulses (NBPs) were observed in [2].

Work done in [3] pioneered the investigation on the effects of interference from natural lightning flashes on wireless communication links at 2.4 GHz. A received signal strength indicator (RSSI) measurement method had been used with 1 m line of sight (LOS) separation. The measured RSSI values were used to simulate bit error rate (BER) for data, audio and video transmissions. The measurement was conducted in Malacca, Malaysia during a rainy day in September 2010. It was concluded that lightning flashes reduce the received power and lead to unreliable communication links.

* Corresponding author at: Ångström Laboratory, Division for Electricity, Department of Engineering Sciences, Uppsala University, Box 534, S-75121, Sweden. Tel.: +46 184715849; fax: +46 184715810.
E-mail addresses: riduan.ahmad@angstrom.uu.se, riduan@utem.edu.my (M.R. Ahmad), monariza.esa@angstrom.uu.se (M.R.M. Esa), Vernon.cooray@angstrom.uu.se (V. Cooray), eryk.dutkiewicz@mq.edu.au (E. Dutkiewicz).

http://dx.doi.org/10.1016/j.epsr.2014.03.022
0378-7796/

In [4,5] the effects of interference from natural lightning flashes on BER of an audio transmission were recorded at 2.4 GHz and 5.8 GHz. The measurement was conducted in Malacca, Malaysia between January and March 2011. The highest recorded BER was 9.9×10^{-1} with the mean BER was 2.07×10^{-2}. The reference measurements under fair weather conditions give a baseline mean BER value at 1.75×10^{-5}. BER values during thunderstorms that higher than 1.75×10^{-5} were interpreted as being interfered by the lightning flashes. Therefore it was concluded that wireless communication system operating at 2.4 GHz was significantly interfered by lightning flashes. However due to the lack of lightning flash events information, the type of CG and IC events that have interfered with the bits transmission could not be identified.

Further work in [6] evaluated possible burst error event to occur during the bits transmission of an audio streaming application at 2.4 GHz. A consecutive lost datagram (CLD) measurement method was used to evaluate the burst error event during 3 heavy thunderstorms between January and March 2011 in Malaysia. It was found that the number of lost packets per burst for all thunderstorms was ranging from 8 to 40 lost packets. However due to the lack of lightning events information, which CG and IC events contributed to the burst error event could not be identified.

In this paper, we are motivated to investigate what type of CG and IC events that possibly have interfered the bits transmission of a wireless communication system operating at 2.4 GHz, which could not be identified by [3–6]. Moreover, it is interesting to study which type of CG and IC events would interfere more severely than the others and contribute to the high BER and burst error events. Recording from the BER measurement system and the electric field change recording system have been synchronized to provide common time stamp information. Lightning waveforms together with the BER and maximum CLD from 3 tropical thunderstorms on November 27, 28, and 29 during 2012 northeastern monsoon in Malaysia were examined and analyzed.

2. Measurement campaign

The measurements were conducted between November and December 2012 during the northeast monsoon period at Observatory Station in Universiti Teknologi Malaysia (UTM), Johor, Malaysia, located at southern part of peninsular Malaysia (1° N, 103° E). The measuring system was situated on a top of a hill that is 132 m above sea level and about 30 km away from Tebrau strait.

A vertically polarized whip antenna was connected through RF coaxial cable to a Levelone WUA-0614 wireless network card [7] attached to a laptop acting as a server. The same laptop acted as a client and was connected to a Cisco WUSB600N wireless network card [8] through a USB cable. At the same time, the laptop acted as a GPS-based time synchronization server and has been synchronized with digital storage oscilloscope (DSO) of the electric field change recording system. The laptop was battery-powered and located inside the observatory station building.

Both the transmitting (whip antenna) and receiving antennas were positioned on a plastic structure (polyvinyl chloride or PVC) 1 m above ground and 3 m from the observatory building. The 'ground' refers to the Earth's surface. A 5 m distance separated the transmitting antenna from the receiving system. Fig. 1 illustrates these configurations. Both the transmitter and the receiver were operating at 2.4 GHz. Adaptive modulations were chosen. Taking 5 m of LOS range into consideration, most probably 64-quadrature amplitude modulation (QAM) was fully utilized.

The application layer at the server of the transmitting system emulated a RealAudio application broadcasting audio content from a multimedia CD-ROM. The average sending data rate was 80 Kbps. The size of the audio data was 1 MB. This data was transmitted using

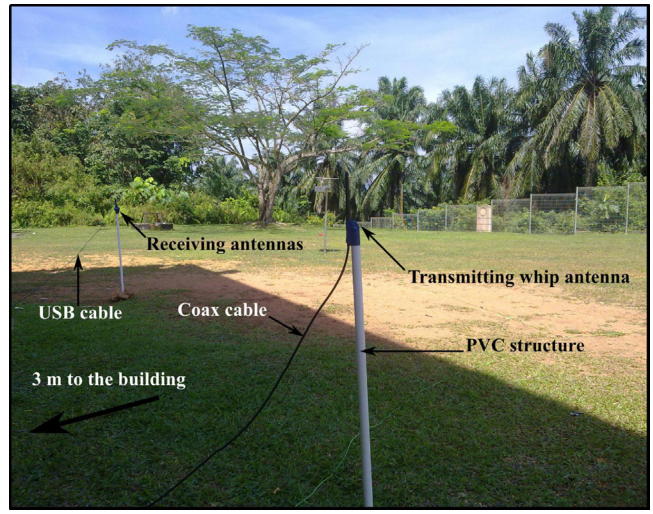

Fig. 1. BER and CLD recording system located 3 m from the observatory station building. The transmitting antenna (vertically polarized whip antenna) was connected to a server laptop through the coaxial cable. The receiving system was connected to a client laptop through the USB cable. Both the transmitting and receiving antennas were positioned on top of a plastic structure (PVC) 1 m from ground and separated by 5 m distance.

real time protocol (RTP) [9] over user datagram protocol/Internet protocol (UDP/IP) as illustrated by Fig. 2 in [5]. The payload type of the RTP was G.729 [10,11]. The total overhead added to a single audio data packet was 40 bytes (from RTP, UDP and IP headers). However datagram segmentation at the UDP layer and packet fragmentation at the IP layer could increase more the total overhead added to the audio data packet. Thus the total number of bytes sent from the server was 1 MB audio data including the total overhead depending on how many datagrams was generated.

Fig. 2. An electric field change recording system located about 9 m from the observatory station building. The buffer circuit was shielded in a metal box during measurements and the captured electrical signal was directed through the 10 m coaxial cable to a DSO located inside the observatory station building.

The Levelone wireless network card forwarded these packets to the receiving system over the wireless communication link by using 802.11n radio interface [12] with a maximum sending rate of 150 Mbps. Distributed coordinated function (DCF) protocol without the request-to-send/clear-to-send (RTS/CTS) mechanism was chosen for the operation of 802.11n radio. The handshaking mechanism was disabled after the hidden node problem was eliminated completely. Also other measures to eliminate hidden node problem had been taken such as providing strong LOS path, shorter Transmitter–Receiver separation and the usage of omni-directional antenna.

The 802.11n radio interface at the receiving system received the transmitted bytes and forwarded them to the client laptop through USB interface with a maximum data rate of 480 Mbps. Forward error correction (FEC) mechanism was used in the 802.11n radio interface to correct any detected error in the received bytes. The frame check sequence (FCS) at the end of each frame detects most of the errors that are not corrected by the FEC scheme. These errors are corrected by retransmissions at the MAC layer. Any bit that cannot be corrected by the FEC and FCS was counted as an error at the IP layer. At the UDP layer, a packet with a certain number of error bytes was considered damaged and discarded. The report of the total number of bytes and packets in error was transmitted to the server after the run time was completed.

The electric field change recording system consisted of a parallel flat plate antenna placed on a metal stand 1.5 m above ground connected via a short 60 cm shielded coaxial cable to a battery-powered buffer circuit. The parallel flat plate antennas together with the buffer circuit (shielded in a metal case as shown in Fig. 2) were positioned about 9 m away from the observatory station building. The top plate of the antenna was connected to the inner conductor of the coaxial cable while the bottom plate was connected to the screening conductor of the coaxial cable. Also the bottom plate was connected directly to the single point grounding system. The buffer circuit was connected to a LeCroy Wave Runner 44Xi-A DSO via 10 m long shielded coaxial cable. The configurations of parallel flat plate antenna and buffer circuit were similar to the configurations used in [13]. The DSO digitized the output of the buffer circuit at 25 Mega Samples/s (20 ns time resolution with 500 ms full window size) and 8-bit vertical resolution with a 100 MHz bandwidth (10 ns impulse width resolution). The DSO was triggered by either positive edge or negative edge of incoming signal with trigger level was varied between 0.1 V and 1 V.

3. Results and analysis

A total of 850 waveforms from the electric field change recording system were recorded and examined during this measurement campaign. Out of these, 94 waveforms of very fine structure were selected which matched perfectly with the timing information of the recorded BER. 78 out of 94 are negative CG (-CG) flash waveforms and the rest are IC flash waveforms. 5 out of 16 IC waveforms are NBP event.

Each BER point corresponds to the number of error bits measured at the receiver for a complete transmission of a 1 MB train of bits from the transmitter. The transmission time for a complete 1 MB train of bits is 800 ms. Each maximum CLD point corresponds to the number of consecutive lost datagram observed at UDP layer. It is an indicator of how severe the occurrence of burst error in wireless communication system. As lightning flash consists events with impulsive activities, it is more likely the nature of interference will be in the form of burst error.

The reference measurements under fair weather conditions give a baseline average BER value at around 1×10^{-5}. Thus BER values during thunderstorms that higher than 1×10^{-5} are interpreted as being interfered by lightning flashes. In general, a communication link for broadcast audio streams is recommended to maintain BER below 1×10^{-3} [14]. In order to increase the accuracy of the analysis and following the recommendation outlined by [14], we have chosen higher baseline BER value at around 1×10^{-3}. Therefore, lightning waveforms which have associated BER values higher than 1×10^{-3} are regarded as the source of interference to the wireless communication system. At frequencies below 10 GHz, attenuation by atmospheric gases and rain may normally be neglected [15]. Thus, we are convinced that the wireless communication system was affected by the thunderstorm alone.

3.1. Interference from cloud-to-ground flashes

Three categories of negative CG flash have been observed to interfere the wireless communication system significantly. The first category of CG flash (Category 1) consists of typical ground flash without PBP and comes with or without chaotic pulses (CP). Fig. 3 shows an example of 4 RSs (with associated SL and dart stepped leader) without CP. A total of 20 waveforms are fall under this category with 8 waveforms consist CP. We observed that all CP were occurred prior to subsequent RS or in between RS. In addition to RS and CP, the second category of CG (Category 2) consists PBP

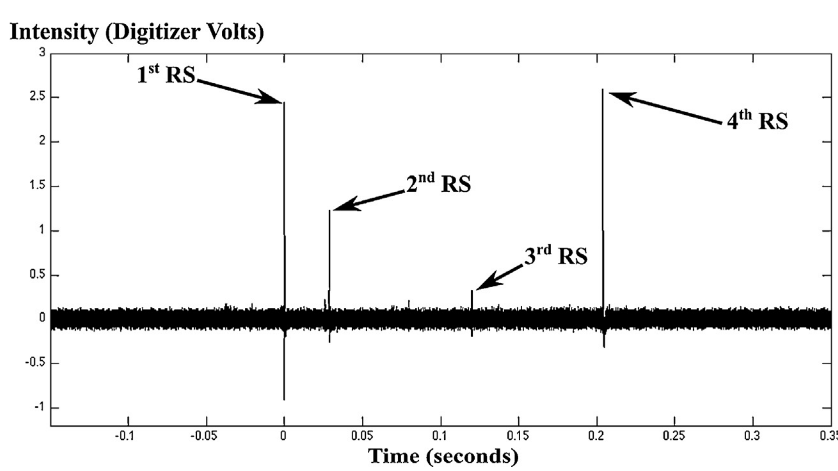

Fig. 3. Activity recorded on 29 November 2012, trace number 84 at 14:45:50, the time window during this measurement was 500 ms with pre-trigger delay of 150 ms. This type of activity is fall under Category 1 of CG flash.

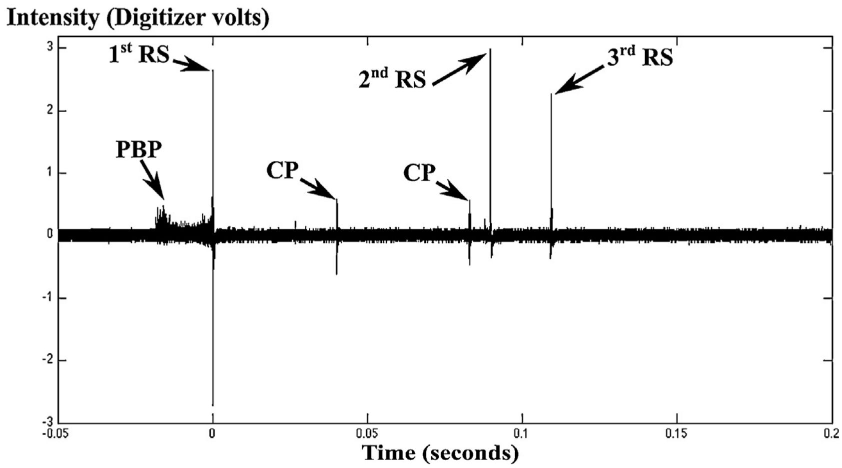

Fig. 4. Activity recorded on 27 November 2012, trace number 230 at 16:22:47, the time window during this measurement was 500 ms with pre-trigger delay of 150 ms. This type of activity is fall under Category 2 of CG flash.

as illustrated in Fig. 4. A total of 38 waveforms are fall under this category with 16 waveforms consist CP.

The third category of CG flash (Category 3) consists of mixed events of large bipolar pulses (Fig. 5a), train of unipolar and bipolar pulses (Fig. 5b), and NBP (Fig. 5c) that were detected together with earlier categories. A total of 20 waveforms are fall under this category. As can be observed from Fig. 5, the large bipolar pulses, NBP and train of pulses were found to occur between and following RS. All the NBP events were observed to have lower intensity compared to the largest RS but comparable to the lowest intensity RS.

The pulse duration of the large bipolar pulses and NBP was observed to be less than 100 μs. The pulse duration of the large bipolar pulses is in the range between 80 and 100 μs while NBP pulse duration is in the range between 5 and 20 μs. In contrast, the duration of the train of unipolar and bipolar pulses was observed to exceed 100 μs. Furthermore, we detected only negative polarity of large bipolar pulses and NBP corresponds to the BER value higher than 1×10^{-3}. On the other hand, the trains of pulses were detected with both polarities.

Correlation of BER and CLD with the number of RS is shown in Figs. 6 and 7, and 10 for all negative CG flash categories tabulated in Table 1. Knowing the correlation of BER and CLD with the number of RS, one will be able to understand how significant microwave radiation from the RS interfering the transmission of bits in wireless communication system. Furthermore, one is able to identify which category of CG interferes more severely the transmission of bits and produces higher burst error. The best-fit correlation lines

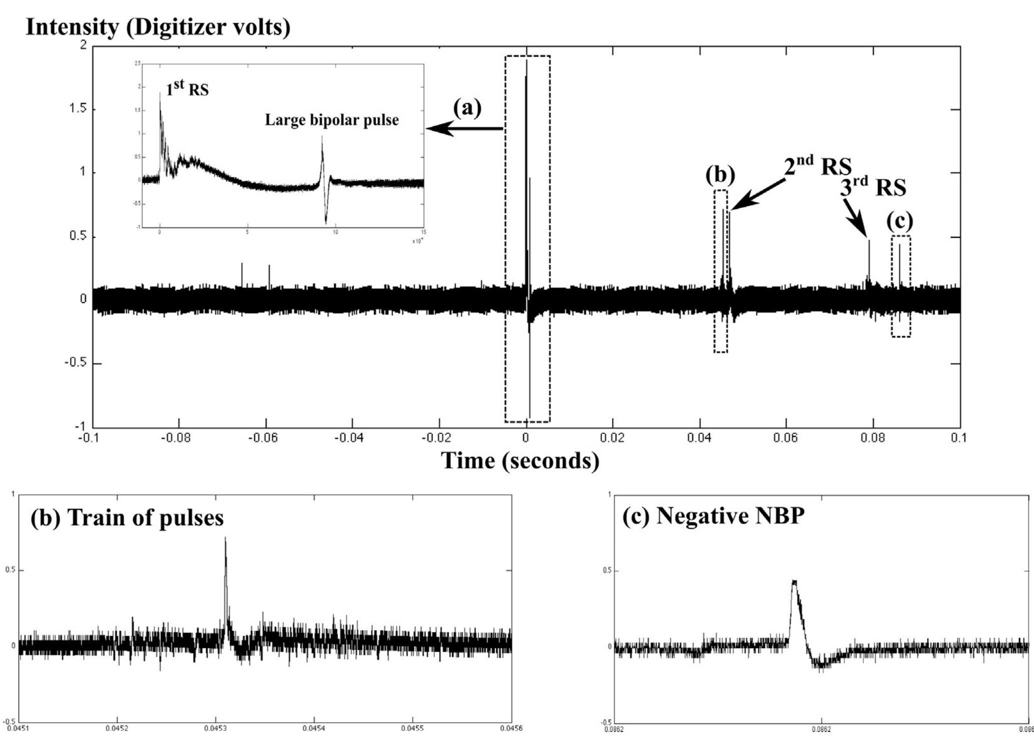

Fig. 5. Activity recorded on 27 November 2012, trace number 147 at 15:46:48, the time window during this measurement was 500 ms with pre-trigger delay of 150 ms. This type of activity is fall under Category 3 of CG flash. As can be seen, the expanded figures show (a) a large bipolar pulse following the first return stroke, (b) train of unipolar and bipolar pulses, and (c) negative NBP (NNBP) following the third return stroke.

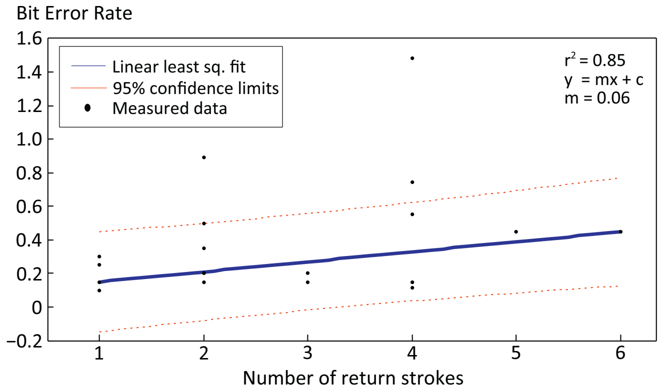

Fig. 6. Linear correlation between BER and the number of RS for Category 1 of CG flash. The BER value has been given in percentage scale, e.g. 1×10^{-2} corresponds to 1.

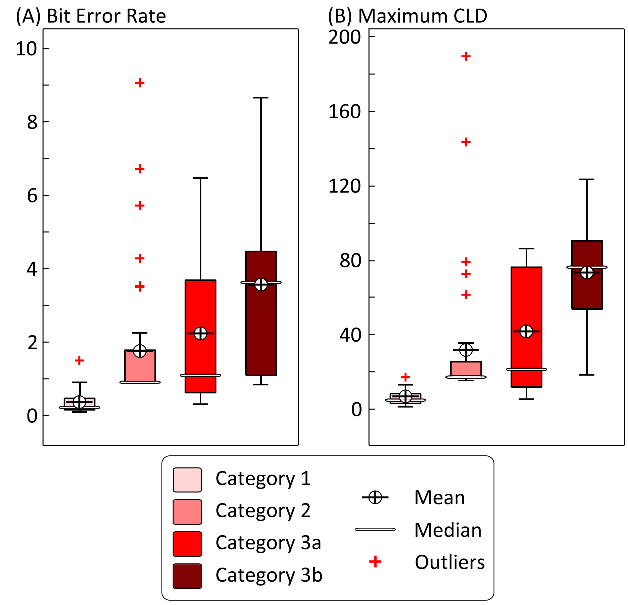

Fig. 8. Statistical distribution of (A) BER and (B) maximum CLD values for Categories 1 to 3 of CG flash. The BER value has been given in percentage scale, e.g. 1×10^{-2} corresponds to 1.

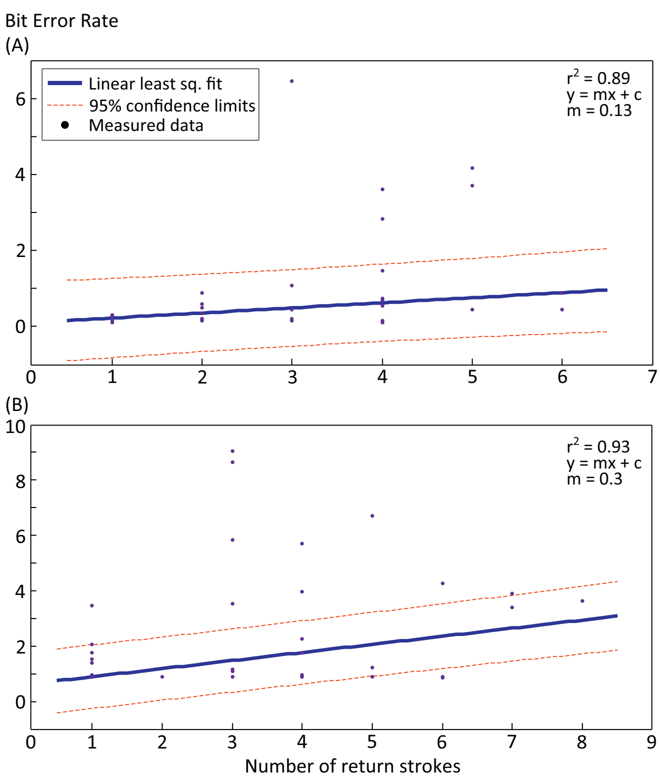

Fig. 7. Linear correlation between BER and the number of RS for (A) Category 4a and (B) Category 4b. The BER value has been given in percentage scale, e.g. 1×10^{-2} corresponds to 1.

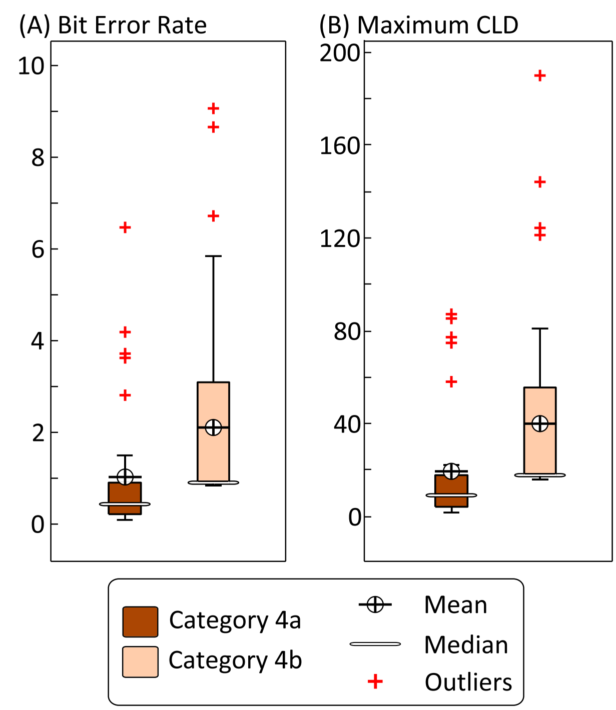

Fig. 9. Statistical distribution of (A) BER and (B) maximum CLD values for Category 4 of CG flash. The BER value has been given in percentage scale, e.g. 1×10^{-2} corresponds to 1.

Table 1
Definitions and explanations of the categories of -CG and IC flashes.

Flash	Category	Events
-CG	1	RSs accompanied by stepped leader, dart (stepped) leaders, and chaotic pulses.
	2	Category 1 event accompanied by PBP event prior the first RS
	3a	Category 1 event accompanied by mixed events consists large bipolar pulses, train of unipolar and bipolar pulses, and NBP.
	3b	Category 2 event accompanied by mixed events consists large bipolar pulses, train of unipolar and bipolar pulses, and NBP.
	4a	Combination of Category 1 and Category 3a events, where PBP event is absent.
	4b	Combination of Category 2 and Category 3b events, where PBP event is present.
IC	1	Typical IC pulses
	2	NBP

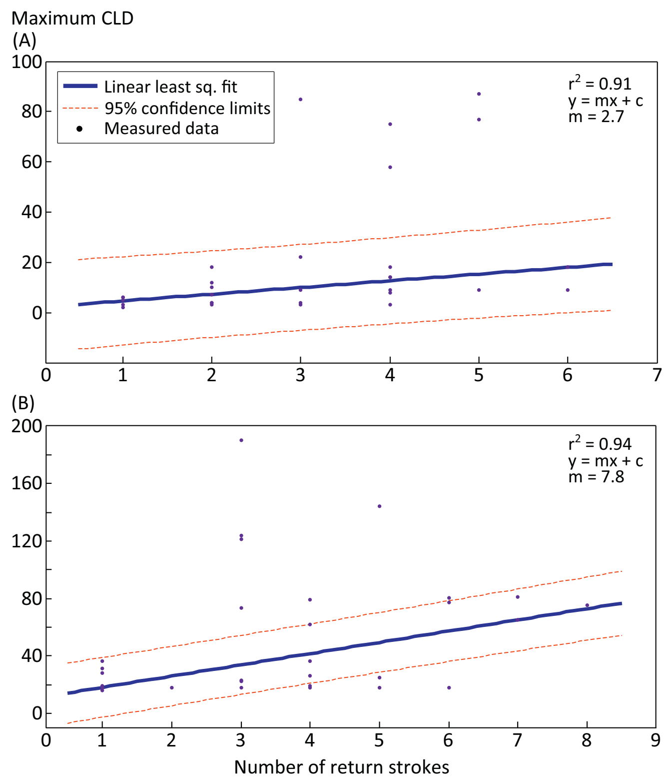

Fig. 10. Linear correlation between maximum CLD and the number of RS for (A) Category 4a and (B) Category 4b of CG flash.

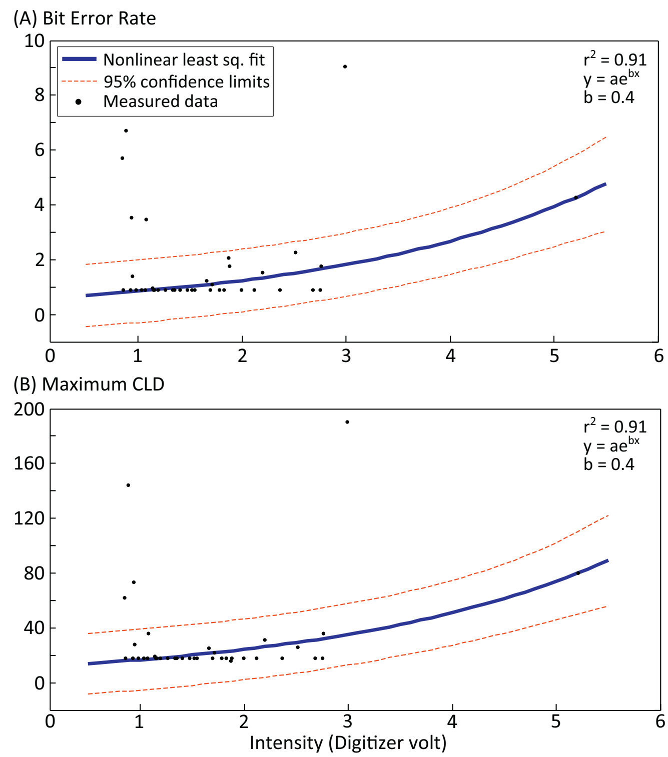

Fig. 11. Nonlinear correlation between (A) BER and the largest intensity, and (B) maximum CLD and the largest intensity, for Category 2 of CG flash. The BER value has been given in percentage scale, e.g. 1×10^{-2} corresponds to 1.

were obtained by using the method of least squares regression. In the case when linear best-fit line could not be obtained and the correlation coefficient requirement cannot be satisfied ($r^2 \geq 0.7$), the method of nonlinear least squares with Gauss–Newton optimization algorithm was applied to obtain the nonlinear best-fit line. The gradient value, m and intercept value, c of the linear best-fit correlation lines can be obtained directly from the first order of polynomial equation, $y(x) = mx + c$. On the other hand, the gradient value, b and intercept value, a of the nonlinear best-fit correlation lines can be obtained directly from the equation of an exponential function, $y(x) = ae^{bx}$.

For Category 1 of CG flash, the BER and the number of RS shows linear correlation with $r^2 = 0.85$ and $m = 0.06$ as shown in Fig. 6. As the number of RS increases from 1 to 6, the BER value increases linearly from 1.5×10^{-3} to 4.5×10^{-3}. We can see clearly from the figure that 95% of the measured BER values are lie within the range of confidence limits of the fit line. Moreover, linear correlation is also observed for Category 4a and Category 4b of CG flash in Fig. 7A and B, respectively. The gradient of Category 4a is much smaller than Category 4b with $m = 0.13$ compared to $m = 0.30$, respectively, but much higher than the gradient of Category 1 of CG flash, $m = 0.06$. As the number of RS increases from 1 to 6, the BER value of Category 4b has increased drastically from 1×10^{-2} to 2.5×10^{-2}, much higher than Category 4a and Category 1 with linear increment from 2×10^{-3} to 8×10^{-3} and from 1.5×10^{-3} to 4.5×10^{-3}, respectively.

Apparently, the BER performance of all CG flash categories becomes worst as the number of RS increases. Further, this observation may suggest that PBP in Category 4b has radiated more significant microwave pulses that interfered with the bits transmission, as a reflection to the much higher gradient and BER values than Category 1 and Category 4a of CG flash. Also, it can be suggested that the mixed events in Category 3 of CG flash radiated significant microwave pulses interfered with the bits transmission

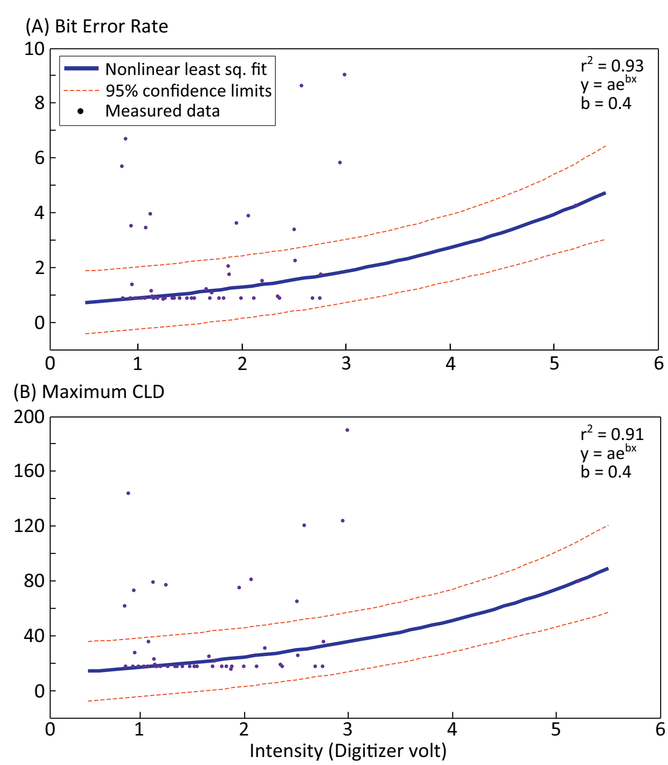

Fig. 12. Nonlinear correlation between (A) BER and the largest intensity, and (B) maximum CLD and the largest intensity, for Category 4b of CG flash. The BER value has been given in percentage scale, e.g. 1×10^{-2} corresponds to 1.

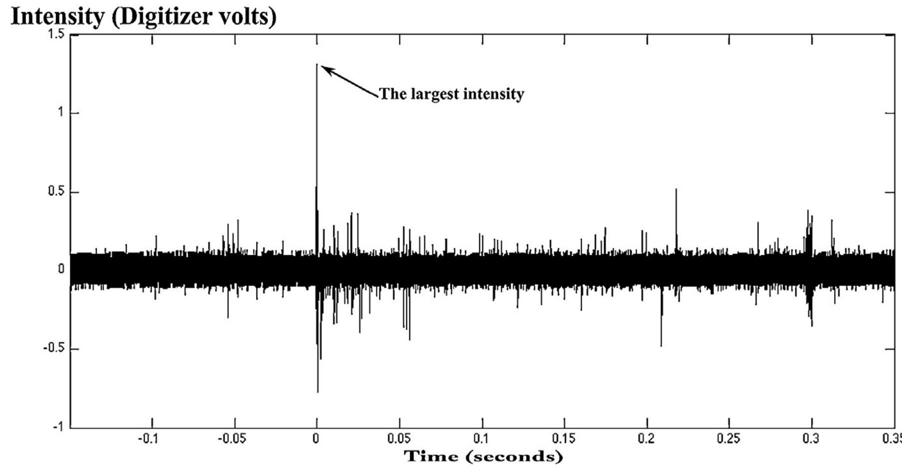

Fig. 13. Activity recorded on 27 November 2012, trace number 257 at 16:51:26, the time window during this measurement was 500 ms with pre-trigger delay of 150 ms. This type of activity is fall under Category 1 of IC.

but not as much as PBP, as a reflection to lower BER values and small difference in gradient values between Category 1 and Category 4a of CG flash.

The statistical distribution of BER values in Fig. 8 supports the reflections of the correlation analysis. Category 1 of CG flash recorded the smallest BER range and also the lowest mean BER value at 3.8×10^{-3} when compared to other categories as evidenced in Fig. 8A. The PBP interfered the bits transmission in the most significant way causes greater BER range and also higher mean BER values at 1.77×10^{-2} and 3.58×10^{-2} for Category 2 and Category 3b of CG flash, respectively. Category 3a recorded only a slightly increase in the mean BER value when compared to Category 2 of CG flash, 2.25×10^{-2} compared to 1.77×10^{-2}, which suggests that the interference from the mixed events is almost comparable to PBP. However, it is important to notice that the range of BER values for Category 3a is much smaller than the range of both Category 2 and Category 3b of CG flash. Moreover, the range and mean BER of Category 4a are much smaller than the range and mean BER of Category 4b as evidenced in Fig. 9A. Therefore, it can be suggested that the mixed events have interfered the bits transmission significantly but not as much as PBP event. Consequently, this may explain why the mixed events in Category 3 of CG flash are suggested to radiate significant microwave pulses but not as much as PBP as revealed from the correlation analysis. Further, we could observe that all the BER values (outliers excluded) of Category 1 of CG flash and Category 4a are below 1.5×10^{-2} while more than 50% of the BER values of Category 2 of CG flash and Category 4b are higher than 1×10^{-2} as evidence from the median values in Figs. 8A and 9A. Most likely PBP event is the strongest source of microwave radiation in CG flash.

A linear correlation between maximum CLD and the number of RS can be seen clearly from Fig. 10A with $r^2 = 0.91$ and from Fig. 10B with $r^2 = 0.94$ for Category 4a and Category 4b, respectively. As the

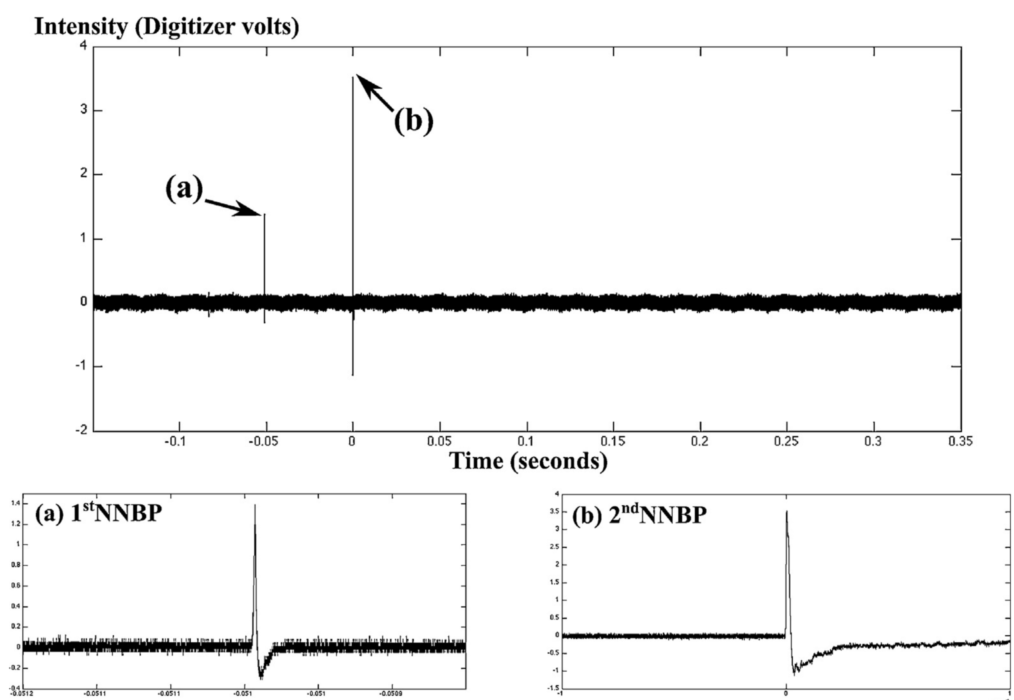

Fig. 14. Activity recorded on 27 November 2012, trace number 54 at 15:14:37, the time window during this measurement was 500 ms with pre-trigger delay of 150 ms. This type of activity is fall under Category 2 of IC. As can be seen, the expanded figure shows (a) the first NNBP and (b) the second NNBP.

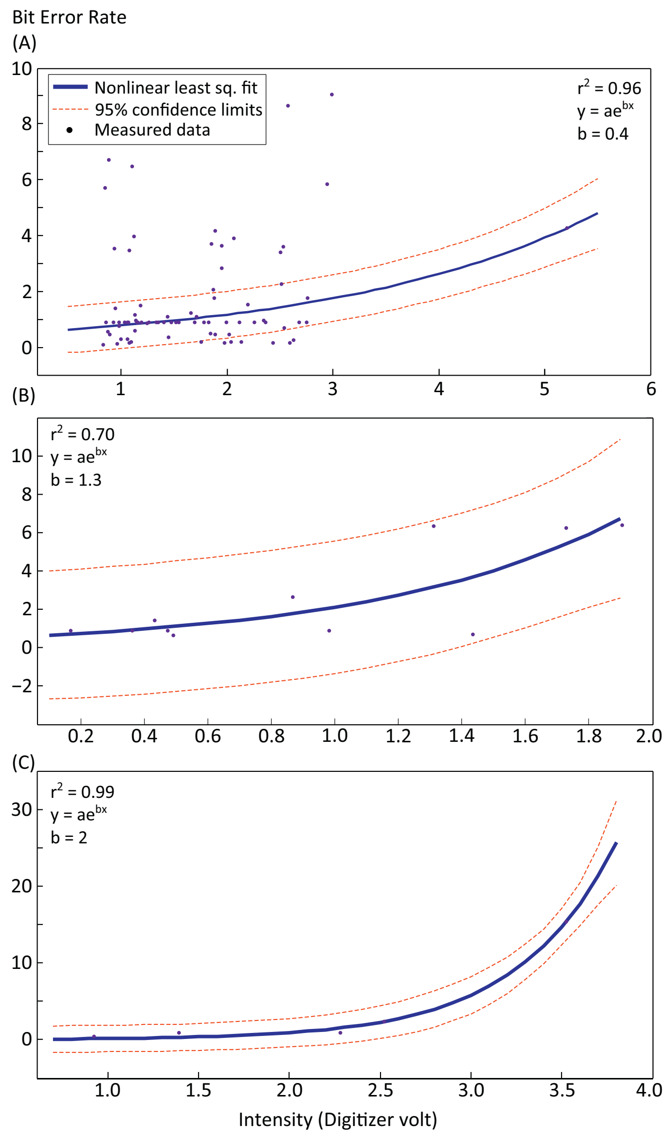

Fig. 15. Nonlinear correlation between BER and the largest intensity for (A) Overall CG flash, (B) Typical IC flash, and (C) NBP. The BER value has been given in percentage scale, e.g. 1×10^{-2} corresponds to 1.

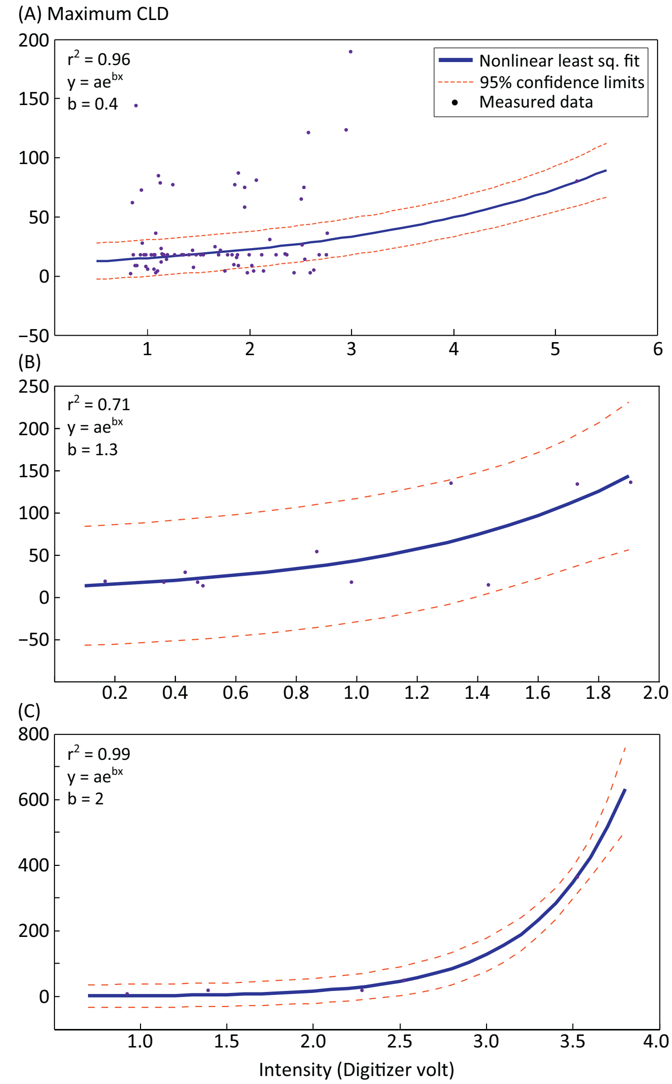

Fig. 16. Nonlinear correlation between maximum CLD and the largest intensity for (A) Overall CG flash, (B) Typical IC flash, and (C) NBP.

number of RS increases from 1 to 6, the number of lost datagram for Category 4a has increased from 5 to 20 datagrams. For Category 4b, the number of lost datagram has increased more drastically and higher than Category 4a, from 20 to 60 datagrams. Moreover, the gradient of Category 4b is estimated to be 7.8, much higher than the gradient of Category 4a at 2.7. Therefore, it could be suggested that Category 4b radiated the most significant microwave pulses, which interfered with the bits transmission and caused the highest burst error. Apparently, correlation analysis reveals that the burst error is more prevalent as the number of RS increases and PBP interfered the bits transmission in the most significant way.

Further, statistical distribution of CLD values in Fig. 8B supports the revelation of correlation analysis where we can observe that Category 3b recorded the highest mean CLD value at 73.78 when compared to Category 3a and Category 1 with 42.09 and 7.15 mean CLD values, respectively. Evidence from Fig. 9B reveals the mean CLD of Category 4b is double the mean CLD of Category 4a. Also, the range and median values of the former category are much larger than the latter category. In addition, we also observe that all the CLD values (outliers excluded) of Category 4a are below 20 datagrams while more than 50% of the CLD values of Category 4b are higher than 20 datagrams and up to 190 datagrams. Evidently, PBP is the strongest source of microwave radiation in CG flash that interfered the bits transmission and consequently increases the BER and CLD values.

Correlation of BER and maximum CLD with the largest intensity is shown in Figs. 11 and 12. The largest intensity here corresponds to the largest amplitude of RS and reflects the distance to the source of radiation. The largest RS intensity is assumed to be inversely proportional to the distance from the source of radiation. Consequently, close radiation source would records much higher intensity RS than the distant radiation source. For Category 2 of CG flash and Category 4b, the BER and the largest intensity shows very good exponential correlation with $r^2 = 0.91$ (Fig. 11A) and $r^2 = 0.93$ (Fig. 12A), respectively. Also, the maximum CLD and the largest intensity shows very good exponential correlation with $r^2 = 0.91$ (Fig. 11B) for the former category and $r^2 = 0.91$ (Fig. 12B) for the latter category. The gradient of Category 2 of CG flash is estimated to be 0.4 for both BER and maximum CLD, the same as the gradient estimated for Category 4b. As the intensity increases from 1 to 5 volts, the BER and maximum CLD values of both categories increases from 1×10^{-2} to 4×10^{-2} and from 20 to 80 datagrams, respectively. This result may suggest that, as the impulsive activity of CG flash events becomes more intense, it would interfere more

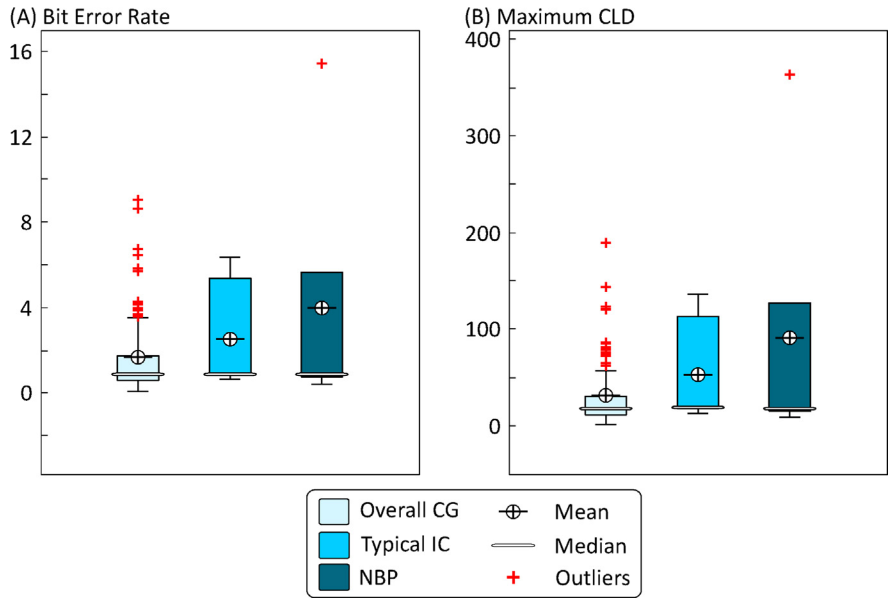

Fig. 17. Statistical distribution of (A) BER and (B) maximum CLD values for overall CG, IC, and NBP flashes. The BER value has been given in percentage scale, e.g. 1×10^{-2} corresponds to 1.

severely with the bits transmission. Also the burst error is more prevalent as the intensity increases.

3.2. Interference from cloud flashes

Two categories of IC have been observed to interfere the wireless communication system significantly. The first category of IC consists typical could flash pulses as shown in Fig. 13. A total of 11 waveforms fall under this category. The second category of IC is a special type of IC known as NBP. A total of 5 waveforms fall under this category. Out of these, 4 are isolated NBP and 1 is in the category of multiple NBP (shown in Fig. 14). All the NBP in this category were observed with large intensity comparable and even larger than the largest RS, unlike the NBP found to occur as part of negative CG flash. Further, we detected 2 positive polarity isolated NBP corresponding to the BER value higher than 1×10^{-3} and the others have the opposite polarity.

Correlation of BER and maximum CLD with the largest intensity is shown in Figs. 15 and 16. The largest intensity here corresponds to the amplitudes of the largest IC pulse and NBP and reflects the distance to the source of radiation. The largest IC and NBP intensities are assumed to be inversely proportional to the distance from the source of radiation. Consequently, close radiation source would record much higher intensity than the distant radiation source. The BER and the largest intensity shows very good exponential correlation with $r^2 = 0.70$ (Fig. 15B) and $r^2 = 0.99$ (Fig. 15C) for the first and second categories of IC, respectively. Also, the maximum CLD and the largest intensity shows very good exponential correlation with $r^2 = 0.71$ (Fig. 16B) and $r^2 = 0.99$ (Fig. 16C) for the first and second categories of IC, respectively. For both BER and maximum CLD, the gradient of the second category of IC is much higher than the first category of IC and overall CG flash category (Figs. 15A and 16A), 2.0 compared to 1.3 and 0.4, respectively.

This result may suggest that, as the impulsive activity of IC gets more intense, it would interfere more severely with the bits transmission. Also the burst error is more prevalent as the intensity increases. Further, the gradient values tell us that the NBP radiated the most intense impulsive microwave pulses, even when compared to all categories of CG flash. The statistical distributions of BER and CLD values in Fig. 17A and B are supporting this finding where the NBP recorded the highest mean BER and CLD values at 4×10^{-2} and 91.60, respectively. On the other hand, the first category of IC recorded mean BER and CLD values at 2.54×10^{-2} and 53.36, respectively, which are found to be higher than the overall CG category with mean BER and CLD values at 1.69×10^{-2} and 31.92, respectively.

4. Discussion and conclusion

Wireless communication system experiences noise and interference even under fair weather condition. However, the interference level is very low and hence the interference effect is negligible in fair weather condition. In this paper, we found that both CG and IC flashes were interfered with the transmission of bits in wireless communication system. The severity of the interference depends mainly on 2 factors namely the number of pulses and the amplitude intensity of the flash. The interference level becomes worst when the number of pulses in a flash increases and the amplitude intensity of pulses in a flash intensifies. When the BER value becomes greater than 1×10^{-3} the signal-to-noise-interference (SINR) ratio drops. Consequently, the performance of wireless communication system starts to degrade significantly. At this level, the effect of interference is noticeable. As the BER value gets higher, the transmission of bits could experience intermittent disturbance due to burst error. When the BER value is greater than 1×10^{-1}, the wireless communication system becomes totally degraded and the communication is expected to be lost. As we can see from the statistical distributions in Figs. 8, 9 and 17, all lightning events recorded BER values lower than 1×10^{-1} except for the NBP event with peak value at 1.54×10^{-1}. Therefore, it can be concluded that during thunderstorms, wireless communication system has experienced mostly intermittent interference due to burst error. Occasionally, in the presence of very intense NBP event, wireless communication system could experience total communication lost.

Studies on frequency spectrum of RS, SL and IC flash in [16] between 100 kHz and 20 MHz, in [17] between 1 kHz and 1 GHz and in [18] between 20 kHz and 20 MHz have revealed that the spectral shape of RS, SL and IC is comparable and the spectral amplitudes are peaked between 1 kHz and 10 kHz and then fall off as $1/f$. At higher frequencies, the spectral amplitude is projected to fall off as $1/f^2$.

However, as discussed in [17], the data points of spectral amplitude above 10 MHz frequency regions were mostly scattered. Thus, it was recommended that more measurements should be done for individual event at higher frequencies to obtain reliable results to resolve the ambiguities in the spectral shape.

In the light of very recent frequency spectrum study in [1], PBP, SL and DL from a negative CG flash have been observed to generate trains of individually resolvable microwave pulses at 1.63 GHz band. The amplitude of the microwave pulses produced by PBP was observed to be more intense than SL and DL. On the other hand, the negative RS was observed to generate noise-like microwave burst instead of individual pulses but with more intense amplitude when compared to PBP. However, the microwave burst of RS lasted only for a few hundreds of microseconds while microwave pulses of PBP lasted longer for several milliseconds duration. This may explain why the interference level from CG flash is significantly higher during the presence of PBP as evidenced in Figs. 8 and 9. The typical PBP train duration is between a few millisecond and tens of milliseconds and thus, most likely that each pulses in the PBP train radiates microwave pulses and interferes with the bits transmission for duration longer than other CG flash events such as RS. Therefore, in CG flash, it can be concluded that PBP is the major source of interference that interfered with the bits transmission and caused the largest burst error.

In IC flash, we found that the typical IC pulses interfered the bits transmission in the same way as PBP and mixed events in CG flash and produced comparable and in some cases higher amount of burst error. On the other hand, NBP has been observed to interfere the bits transmission more severely than typical IC and CG flashes as evidenced in Figs. 15–17. Recent work in [2] revealed that NBP has produced noise-like microwave burst lasted for several microseconds at 2.4 GHz band. It is interesting to wonder how a single NBP pulse could produce very intense microwave radiation pulses that could interfere the bits transmission severely. If we consider the very recent proposal put forward in [19] to be true that NBP discharge is the result of relativistic electron avalanches mechanism rather than conventional leader discharge. Then, the spectral amplitude of the resultant radiation field would be peaked at around 1 GHz as estimated in [20]. This may explain our finding and provide logical reason why a single NBP pulse could produce very intense microwave burst at 2.4 GHz band and caused the most severe burst error to wireless communication system.

Acknowledgements

This paper is a revised and extended version of contribution [4] kindly presented by the first author at the 2012 International Conference on Lightning Protection (ICLP). We would like to thank the participants for their helpful comments and suggestions. Research work in this paper was funded by Ministry of Higher Education Malaysia and Anna Maria Lundin Foundation (Småland Nation). Participation of Vernon Cooray was funded by the fund from the B. John F. and Svea Andersson donation at Uppsala University. We would like to thank Assoc. Prof. Dr. Zulkurnain Abd. Malek, Dr. Azlinda, Ms. Zaini, Mr. Kamyar and Mr. Behnam, from IVAT, UTM, Malaysia for the supports during the measurement campaign.

References

[1] D. Petersen, W. Beasley, Microwave radio emissions of negative cloud-to-ground lightning flashes, Atmos. Res. 135–136 (2014) 314–321.
[2] M.R. Ahmad, M.R.M. Esa, V. Cooray, Narrow bipolar pulses and associated microwave radiation, in: Proc. of Progress In Electromagnetics Research Symposium (PIERS), Stockholm, Sweden, August 12–15, 2013, pp. 1087–1090.
[3] M.R. Ahmad, M. Rashid, M.H.A. Aziz, M.M. Esa, V. Cooray, M. Rahman, E. Dutkiewicz, Analysis of lightning-induced transient in 2.4 GHz wireless communication system, in: Proc. of IEEE International Conference on Space Science and Communication (IconSpace), Penang, Malaysia, July 12–13, 2011, pp. 225–230.
[4] M.R. Ahmad, M.R.M. Esa, M. Rahman, V. Cooray, Measurement of bit error rate at 2.4 GHz due to lightning interference, in: Proc. of International Conference on Lightning Protection (ICLP), Vienna, Austria, September 2–7, 2012, pp. 1–4.
[5] M.R. Ahmad, M.R.M. Esa, M. Rahman, V. Cooray, E. Dutkiewicz, Lightning interference in multiple antennas wireless communication systems, J. Light. Res. 4 (2012) 155–165.
[6] M.R. Ahmad, M.R.M. Esa, V. Cooray, E. Dutkiewicz, Performance analysis of audio streaming over lightning-interfered MIMO channels, in: Proc. of International Symposium on Communications and Information Technologies (ISCIT), Gold Coast, Australia, October 2–5, 2012, pp. 513–518.
[7] Levelone Wireless Nano USB Network Adapter WUA-0614 Datasheet. Available: http://global.level1.com/datasheet/WUA-0614-V2_SPEC_EN.pdf
[8] Linksys Ultra Rangeplus Dual-band Wireless-N USB Network Adapter WUSB600N Specifications (Network Adapter), CNET Review Web Site. Available: http://reviews.cnet.com/adapters-nics/linksys-ultra-rangeplus-dual/4507-3380_7-32816737.html
[9] H. Schulzrinne, S. Casner, R. Frederick, V. Jacobson, RTP: A Transport Protocol for Real-Time Applications, IETF RFC 3550 Standard 2003. Available: http://tools.ietf.org/html/rfc3550
[10] Implementors' Guide for ITU-T Rec. G. 729 (2007): Coding of Speech at 8 kbit/s Using CS-ACELP, Telecommunication Standardization Sector of ITU Series G: Transmission Systems and Media, Digital Systems and Networks 2009. Available: http://www.itu.int/rec/T-REC-G.Imp729-200911-I/en
[11] IEEE standard for information technology: Telecommunications and information exchange between systems: Local and metropolitan area networks: Specific requirements, Supplement to carrier sense multiple access with collision detection (CSMA/CD) access method and physical layer specifications: Physical layer parameters and specifications for 1000 Mb/s operation over 4-pair of category 5 balanced copper cabling type 1000BASE-T, IEEE standard 802.3ab 1999.
[12] IEEE standard for information technology: Local and metropolitan area networks: Specific requirements: Part 11: Wireless LAN medium access control (MAC) and physical layer (PHY) specifications amendment 5: Enhancements for higher throughput, IEEE standard 802.11n 2009.
[13] M.R.M. Esa, M.R. Ahmad, V. Cooray, Wavelet analysis of the first electric field pulse of lightning flashes in Sweden, Atmos. Res. 138 (2014) 253–267.
[14] Y. Chen, T. Farley, N. Ye, QoS requirements of network applications on the Internet, J. Inform. Knowl. Syst. Manage. 4 (2004) 55–76.
[15] Recommendation ITU-R P.618-9: Propagation Data and Prediction Methods Required for the Design of Earth-Space Telecommunication Systems, Radiocommunication Sector of ITU Series P: Radiowave Propagation 2009. Available: http://www.itu.int/rec/R-REC-P.618-10-200910-I/en
[16] C.D. Weidman, E.P. Krider, M.A. Uman, Lightning amplitude spectra in the interval from 100 kHz to 20 MHz, Geophys. Res. Lett. 8 (1981) 931–934.
[17] D.M. Le Vine, Review measurements of the RF spectra of radiation from lightning, Meteorol. Atmos. Phys. 37 (1987) 195–204.
[18] U. Sonnadara, V. Cooray, M. Fernando, The lightning radiation field spectra of cloud flashes in the interval from 20 kHz to 20 MHz, IEEE Trans. Electromagn. Compat. 48 (1) (2006) 234–239.
[19] V. Cooray, G. Cooray, T. Marshall, S. Arabshahi, J. Dwyer, H. Rassoul, Electromagnetic fields of a relativistic electron avalanche with special attention to the origin of lightning signatures known as narrow bipolar pulses, Atmos. Res. (2014) (in press).
[20] V. Cooray, G. Cooray, Electromagnetic radiation field of an electron avalanche, Atmos. Res. 117 (2012) 18–27.